Received: 13 September 2019 | Revised: 22 November 2019 | Accepted: 3 December 2019

DOI: 10.1096/fj.201902347R

RESEARCH ARTICLE

THE FASEB JOURNAL

Mouse brain proteomics establishes MDGA1 and CACHD1 as in vivo substrates of the Alzheimer protease BACE1

Jasenka Rudan Njavro[1,2] | Jakob Klotz[1,2] | Bastian Dislich[1,3] | Johanna Wanngren[4] | Merav D. Shmueli[1,2,5] | Julia Herber[1,2] | Peer-Hendrik Kuhn[6] | Rohit Kumar[1,7,8] | Thomas Koeglsperger[1,8] | Marcus Conrad[9] | Wolfgang Wurst[9,10,11,12] | Regina Feederle[12,13,14] | Andreas Vlachos[15,16] | Stylianos Michalakis[17] | Peter Jedlicka[18,19,20] | Stephan A. Müller[1,2] | Stefan F. Lichtenthaler[1,2,12]

[1]German Center for Neurodegenerative Diseases (DZNE), Munich, Germany

[2]Neuroproteomics, School of Medicine, Klinikum rechts der Isar, Technical University of Munich, Munich, Germany

[3]Institute of Pathology, University of Bern, Switzerland

[4]Division of Neurogeriatrics, Department of NVS, Center for Alzheimer Research, Karolinska Institutet, Stockholm, Sweden

[5]Department of Immunology, The Weizmann Institute of Science, Rehovot, Israel

[6]Institute of Pathology, Technical University of Munich, Munich, Germany

[7]School of Medicine, Klinikum rechts der Isar, Technical University of Munich, Munich, Germany

[8]Department of Neurology, Ludwig Maximilian University of Munich, Munich, Germany

[9]Institute of Developmental Genetics, Helmholtz Zentrum München, Neuherberg, Germany

[10]Genome Engineering, German Center for Neurodegenerative Diseases (DZNE), Munich, Germany

[11]Developmental Genetics, School of Life Sciences Weihenstephan, Technical University of Munich, Freising, Germany

[12]Munich Cluster for Systems Neurology (SyNergy), Munich, Germany

[13]German Research Center for Environmental Health, Institute for Diabetes and Obesity, Monoclonal Antibody Core Facility, Helmholtz Zentrum München, Neuherberg, Germany

[14]Core Facility Monoclonal Antibodies, German Center for Neurodegenerative Diseases (DZNE), Munich, Germany

[15]Department of Neuroanatomy, Institute of Anatomy and Cell Biology, Faculty of Medicine, University of Freiburg, Germany

[16]Center for Basics in Neuromodulation (NeuroModulBasics), Faculty of Medicine, University of Freiburg, Germany

[17]Department of Ophthalmology, Ludwig Maximilian University of Munich, Munich, Germany

[18]Faculty of Medicine, ICAR3R - Interdisciplinary Centre for 3Rs in Animal Research, Justus-Liebig-University, Giessen, Germany

[19]Neuroscience Center, Institute of Clinical Neuroanatomy, Goethe University, Frankfurt am Main, Germany

[20]Frankfurt Institute for Advanced Studies, Frankfurt am Main, Germany

Abbreviations: Aβ, amyloid beta; AD, Alzheimer's disease; ADAM, a disintegrin and metalloproteases; APP, amyloid precursor protein; BACE1, beta-site APP cleaving enzyme 1; BACE1 coKO, BACE1 conditional knockout; BACE2, beta-site APP cleaving enzyme 2; CACHD1, VWFA and cache domain-containing protein 1; CHL1, close homolog of L1; CTF, C-terminal fragment; DMSO, dimethyl sulfoxide; FLP, flippase; FRT, flip recombinase target; LTP, long-term potentiation; MDGA1, MAM domain-containing glycosylphosphatidylinositol anchor protein 1; mIPSC, miniature inhibitory postsynaptic currents; NRG1, neuregulin-1; NLGN2, neuroligin-2; SEZ6, seizure protein 6; SILA, stable isotope labeling with amino acids; SPPL3, signal peptide peptidase-like 3; VEGFR1, vascular endothelial growth factor receptor 1.

Jasenka Rudan Njavro, Jakob Klotz, Bastian Dislich, and Johanna Wanngren shared first authors.

Correspondence
Stefan F. Lichtenthaler, German Center for Neurodegenerative Diseases (DZNE), Munich, Germany.
Email: Stefan.Lichtenthaler@dzne.de

Funding information
Deutsche Forschungsgemeinschaft (DFG), Grant/Award Number: EXC 2145 SyNergy, project ID 390857198, JE 528/6-1 and FOR 2290; BMBF Bundesministerium für Bildung und Forschung, Grant/Award Number: CLINSPECT-M; Swedish Society of Medical Research, Grant/Award Number: 123; Alzheimer Forschung Initiative (AFI), Grant/Award Number: 15038

Abstract

The protease beta-site APP cleaving enzyme 1 (BACE1) has fundamental functions in the nervous system. Its inhibition is a major therapeutic approach in Alzheimer's disease, because BACE1 cleaves the amyloid precursor protein (APP), thereby catalyzing the first step in the generation of the pathogenic amyloid beta (Aβ) peptide. Yet, BACE1 cleaves numerous additional membrane proteins besides APP. Most of these substrates have been identified in vitro, but only few were further validated or characterized in vivo. To identify BACE1 substrates with in vivo relevance, we used isotope label-based quantitative proteomics of wild type and BACE1-deficient (BACE1 KO) mouse brains. This approach identified known BACE1 substrates, including Close homolog of L1 and contactin-2, which were found to be enriched in the membrane fraction of BACE1 KO brains. VWFA and cache domain-containing protein 1 (CACHD)1 and MAM domain-containing glycosylphosphatidylinositol anchor protein 1 (MDGA1), which have functions in synaptic transmission, were identified and validated as new BACE1 substrates in vivo by immunoblots using primary neurons and mouse brains. Inhibition or deletion of BACE1 from primary neurons resulted in a pronounced inhibition of substrate cleavage and a concomitant increase in full-length protein levels of CACHD1 and MDGA1. The BACE1 cleavage site in both proteins was determined to be located within the juxtamembrane domain. In summary, this study identifies and validates CACHD1 and MDGA1 as novel in vivo substrates for BACE1, suggesting that cleavage of both proteins may contribute to the numerous functions of BACE1 in the nervous system.

KEYWORDS

gamma-secretase, inhibitory synapse, retina, secretase, SILAC

1 | INTRODUCTION

Ectodomain shedding of membrane proteins is a basic cellular process controlling the communication between cells, including in the brain.[1] Upon shedding, the extracellular domain of a membrane protein is proteolytically cleaved off and released from cells. The contributing proteases, referred to as sheddases, are mostly themselves membrane-bound enzymes and often do not only cleave a single substrate, but numerous different ones. Among the sheddases with multiple substrates are rhomboids,[2-4] a disintegrin and metalloproteases (ADAM),[5-8] signal peptide peptidase-like 3 (SPPL3)[9,10] and the beta-site APP cleaving enzymes (BACE) BACE1[11-15] and BACE2.[12,16]

Beta-site APP cleaving enzyme 1 was initially identified as the enzyme that cleaves the amyloid precursor protein (APP) at the β-secretase cleavage site.[17] As a result, it sheds the APP ectodomain and catalyzes the first step in the generation of the amyloid beta (Aβ) peptide which is seen as a key pathogenic agent in the early steps of Alzheimer's disease (AD) pathogenesis.[18] Thus, BACE1 inhibition is a major therapeutic approach for AD and several BACE1-targeting inhibitors have been advanced into phase 3 clinical trials.[19] However, several side effects were observed in some phase 3 trials, such as psychiatric symptoms and increased falls,[20-22] which may be mechanism-based because BACE1 does not only cleave APP, but has multiple additional substrates with functions in the nervous system.[23] Moreover, BACE1 KO mice show several phenotypes, revealing a fundamental function for BACE1 in the nervous system. For several phenotypes, the contributing substrates have been identified. For example in mice, loss of BACE1 cleavage of neuregulin-1 (NRG1) induces hypomyelination and defects in muscle spindle formation and maintenance.[24-26] Loss of cleavage of seizure protein 6 (SEZ6) leads to defects in dendritic spine density and reduced long-term potentiation (LTP)[27-29] and lack of cleavage of the close homolog of L1 (CHL1) reduces the length of the infrapyramidal bundle, an anatomical structure in the hippocampus,[30,31] whereas loss of Jagged-1 cleavage reduces neurogenesis and increases astrogenesis in mouse brain development.[32] For several other phenotypes observed in BACE1 KO mice, such as memory deficits,[33-36] neurochemical deficits[37] or postnatal lethality, and growth retardation,[38] the contributing substrate(s) are not yet known.

This is, at least partly, due to lack of knowledge, which additional BACE1 substrates are relevant in vivo. While more than 40 BACE1 substrates have been identified, mostly in cell lines and primary neurons,[11-14] only few of them were further validated or characterized in vivo.[11,23,39]

Thus, here we investigated BACE1 substrates in vivo, using the spike-in Stable Isotope Labeling with Amino acids (SILA) mouse technique combined with quantitative proteomics and analyzed BACE1 KO brains. We identified several known and new BACE1 substrates to be enriched in the brain membrane fractions of BACE1 KO mice. Furthermore, we validated the membrane proteins "MAM domain-containing glycosylphosphatidylinositol anchor protein 1" (MDGA1) and "VWFA and cache domain-containing protein 1" (CACHD1) as BACE1 substrates in vitro and in vivo and determined their cleavage site by BACE1, which was found to be located in the juxtamembrane domain at a short distance from the substrates' transmembrane domain.

2 | EXPERIMENTAL PROCEDURES

2.1 | Mouse strains

The following mouse strains were used: wild type (WT) C57BL/6 (Charles River, Wilmington, MA, USA), BACE1 conditional knockout (BACE1 coKO; described below) and BACE1 KO (Jackson Laboratory, Bar Harbor, ME, USA, strain B6.129-Bace1tm1Pcw/J).[40] These BACE1 KO mice were generated with the use of C57BL/6J blastocysts, with the chimeric animals being crossed to C57BL/6 mice, and then backcrossed for seven generations. Heavy labeled SILAC mouse brains (Lys ^{13}C, 97%) were purchased from Silantes Gmbh, Munich, Germany. All animals were maintained with food and water ad libitum and on a 12/12 h light-dark cycle. The procedures and protocols were in accordance with the European Communities Council Directive (86/609/EEC) and approved by the Ludwig-Maximilians-Universität München and the government of Upper Bavaria.

2.2 | Membrane preparation of the brain

Mouse brains (200 mg) were homogenized in 1 mL high salt buffer (2 M NaCl, 10 mM HEPES/NaOH, pH 7.4, and 1 mM EDTA, in ddH2O, supplemented with protease inhibitor mix, 1:100, Roche) using a tissue homogenizer (Omni International, Kennesaw, GA, USA) at maximum speed for 60 s and afterward centrifuged at 17 000 *g* for 15 minutes at 4°C (every washing step included the same centrifugation step). Cell pellet was washed two times with carbonate buffer (0.1 M Na_2CO_3, pH 11.3, and 1 mM EDTA, in ddH_2O), once with urea buffer (5 M urea, 100 mM NaCl, 10 mM HEPES, pH 7.4, and 1 mM EDTA, in ddH_2O) and two more times with Tris-HCl (0.1M TRIS/HCL, pH 7.6, in ddH_2O). Membrane pellet was resuspended in 50 µL SDT-lysis buffer (2% (w/v) SDS, 100 mM TRIS/HCl pH 7.6, 0.1M DTT, in ddH_2O) and incubated for 5 minutes at 95°C.

2.3 | Proteomic analysis of brain membrane fractions of BACE1 KO mice

For the proteomic analysis of the brain membrane fraction of BACE1 KO mice, the brains of BACE1 KO mice and their WT littermates at postnatal day 3 (P3) were dissected. In order to allow a *P* value–based statistical analysis of the data, three knockout and three WT mice were analyzed, all from the same litter that resulted from the mating of a heterozygous BACE1 KO (−/+) male with a heterozygous BACE1 KO (−/+) female. The brain tissue was homogenized in high salt buffer for membrane preparation as described above. In addition, P3 brains from mice stable isotope labeled by amino acids (SILA) with ^{13}C lysine (Silantes Gmbh) were homogenized in the same buffer. After a protein assay, the homogenates of SILA mouse brains were spiked into the samples of BACE1 KO and WT mice using a 1:1 protein ratio. The brain homogenates with the spike-in were subjected to membrane preparation as described above.

Membrane pellets were lysed in SDT buffer and 100 µg of proteins were subjected to filter aided sample preparation (FASP)[41] as previously described with some modifications. Briefly, Vivacon 500 ultrafiltration columns with a cutoff of 30 kDa (Sartorius, Goettingen, Germany) were used. Since spike-in brain samples were labeled with ^{13}C lysine, only LysC was used for proteolytic digestion. Peptides were enriched and desalted using self-packed stop and go extraction (STAGE) tips with C18 material (EMPORE, 3M, Seefeld, Germany) as previously described.[42] Peptides were dissolved in a 250 mM Britton and Robinson (B&R) buffer with a pH of 11 and a peptide fractionation was performed with SAX STAGE tips (Empore, 3M) as previously described.[43] Briefly, six fractions were eluted using B&R buffers with pH 11, pH 8, pH 6, pH 5, pH 4, and pH 3. Peptides were desalted again with C18 STAGE tips, dissolved in 0.1% formic acid and subjected to liquid chromatography tandem mass spectrometry analysis (LC-MS/MS).

Two technical replicates were acquired for each of the peptide fractions and samples. For one biological replicate, the peptide yield was too low and only one technical replicate was measured. Peptides were separated on an in-house packed 15 cm C18 column (ID: 75 µm, 2.4 µm Reprosil-Pur C18 AQ, Dr Maisch GmbH) using an Easy nLC II (Proxeon, part of Thermo Fisher Scientific, USA) nanoHPLC system with a binary gradient of water (A) and acetonitrile (B) supplemented

with 0.1% formic acid at a flow rate of 400 nL/min (0 minutes, 8% B; 145 minutes, 25% B; 227 minutes, 45% B). The LC was coupled online via a nano electrospray ion source to a LTQ Velos Pro Orbitrap mass spectrometer (Thermo Fisher Scientific, USA). Full MS spectra were acquired at a resolution 60 000 covering a scan range of 300-2000 m/z. The 14 peptide ions with the highest intensities in each scan cycle were chosen for collision induced dissociation in the ion trap (min signal: 1000; isolation width: 2 m/z; normalized collision energy: 35%; activation q: 0.25; activation time: 10 ms; wideband activation applied). A dynamic exclusion of 120 s was applied for precursor selection.

The peptide cleavage assay was analyzed on an Easy nLC 1000 nanoUHPLC coupled online to a Velos pro Orbitrap for MDGA1 and a Q-Exactive mass spectrometer (Thermo Fisher Scientific, USA) for CACHD1 using in-house packed 30 cm C18 column (ID: 75 µm, 1.9 µm Reprosil-Pur C18 AQ, Dr Maisch GmbH). A gradient of 35 minutes at 250 nL/min and 50°C column temperature was applied. The Velos pro Orbitrap was used with similar setting as described above. The Q-exactive mass spectrometer was used with following settings: Full MS spectra were acquired at a resolution of 70 000 covering a scan range of 300 to 1400 m/z. The 10 peptides with the highest intensities were chosen for peptide fragmentation (automatic gain control: 5 E + 3 ions; isolation width: 2 m/z; maximum trapping time: 100-200 ms; resolution: 17 500).

2.4 | Proteomic data analysis

The data were analyzed with the software Maxquant (maxquant.org, Max-Planck Institute Munich, Germany) version 1.6.3.3.[44] The MS data were searched against a reviewed canonical fasta database of *Mus musculus* from UniProt (download: November the 5th 2018, 17005 entries). Trypsin was defined as the protease. Two missed cleavages were allowed for the database search. The option first search was used to recalibrate the peptide masses within a window of 20 ppm. For the main search peptide and peptide fragment mass tolerances were set to 4.5 and 20 ppm, respectively. Carbamidomethylation of cysteine was defined as static modification. Acetylation of the protein N-term as well as oxidation of methionine was set as variable modifications. The false discovery rate (FDR) for both peptides and proteins was adjusted to less than 1%. The "match between runs" option was enabled with a matching window of 1.5 minutes. Relative quantification based on labeled lysine of proteins required at least one ratio counts of unique peptides. Only unique peptides were used for quantification.

To identify peptides of the peptide cleavage assay a database search against the full-length peptides using unspecific cleavage was applied using Maxquant (version 1.5.3.12 or 1.6.6.0). Peptides with a score higher than 40 were considered as potential hits. The peaks of the cleavage products and the full-length peptides were extracted in XCalibur to visualize changes between incubation with recombinant BACE1, BACE1, and inhibitor C3, as well as incubation without BACE1.

2.5 | Statistical analysis

The protein quantification data of Maxquant was further processed in Perseus.[45] The normalized heavy to light protein ratios were log2 transformed. Afterwards, the log2 ratios of technical replicates were averaged and average protein log2 fold changes were calculated between BACE1 KO and WT samples. A two-sided Student's *t* test was applied to evaluate the significance of proteins with changed abundance. In addition, permutation-based FDR estimation was used.[46]

Immunoblots of membrane fractions of the brain were performed with three additional biological replicates. Immunoblots of neurons were done using at least two different neuronal preparations divided in up to six experiments for each condition within one preparation. This yielded 9 to 16 independent experiments per each condition. Statistical testing was performed using Mann-Whitney U test with the significance criteria of $P < .05$.

2.6 | Western blotting and antibodies

To detect the soluble form of MDGA1, enrichment with Concanavalin A (ConA) beads (Sigma, Merck, Darmstadt, Germany; C7555) was used. According to the protein lysate, the amount of conditioned media was used for pull-down (sample with the lowest protein amount had maximum of 900 µL of conditioned media) together with the 50 µL of prewashed ConA (washed two times in PBS). Each washing step included 5 minutes rotation at room temperature and centrifugation step at 2500 *g* and 4°C. The samples were rotating overnight at 4°C, and then washed additional two times with PBS. For MDGA1, twenty-five microliters of nonreducing sample buffer (without β-mercaptoethanol) was added to the beads and incubated for 5 minutes, at 95°C. Other samples were diluted in regular Laemmli buffer and incubated for 5 minutes at 95°C. For sample separation, 8% or 12% SDS-polyacrylamide gels were used. Polyvinylidene difluoride (PVDF) transferred membranes were incubated with primary antibody overnight at 4°C, while the secondary antibody for 1 hour at room temperature.

Primary antibodies used: APP (Millipore, Merck; 22C11, dilution 1:1000), BACE1 (Robert Vassar, Northwestern University, Chicago, IL, USA; 3D5, dilution 1:1000), CHL1 (R&D Systems, Minneapolis, MN, USA; AF2147, dilution

1:1000), CNTN2 (R&D Systems; AF4439, dilution 1:1000), β-actin (Sigma, Merck; AC-74, A5316, dilution 1:1000), Calnexin (Enzo Life Sciences, Germany; ADI-SPA-860, dilution 1:1000), HA (Covance, Princeton, NJ, USA; MMS-101P, dilution 1:1000), NrCAM (Abcam, Cambridge, UK; ab24344, dilution 1:1000), and SEZ6 (dilution 1:10 of primary hybridoma supernatant).[47] Monoclonal anti-CACHD1 antibody CACHI 15H10 (rat IgG1/k) (dilution 1:10 of primary hybridoma supernatant) was generated by immunization of Lou/c rats with the peptide NLENDRDERDDDSHEDR (intracellular part of murine and human CACHD1) using standard procedures.[48] Monoclonal anti-MDGA1 antibody DGA 21E3 (rat IgG2a/k) (dilution 1:10 of primary hybridoma supernatant) was generated by immunization of Lou/c rats with native recombinant, C-terminally BAP-HIS-tagged murine MDGA1 ectodomain spanning amino acids 20-925 which was lentivirally transduced and overexpressed in HEK293T via a Gal4-UAS expression system and purified via metal affinity chromatography. Secondary antibodies used: HRP-coupled anti-goat (Santa Cruz, Heidelberg, Germany, sc-2020, dilution 1:5000), anti-mouse (Promega, Mannheim, Germany, W402B, dilution 1:10 000), anti-rabbit (Promega, W401B, dilution 1:10 000) and anti-rat (Santa Cruz, sc-2006, dilution 1:5000).

2.7 | Preparation of primary mouse cortical and hippocampal neurons

Mouse cortical and hippocampal neurons were obtained from the embryonic day 16 cortex or hippocampus, cleaned from the meninges and collected in cold HBSS (Thermo Fisher Scientific, Darmstadt, Germany; 24020-091) as described.[49,50] Tissue was then incubated for 15 to 20 minutes at 37°C in digestion medium (9.7 ml Dulbecco's Modified Eagle Medium (DMEM) high glucose with GlutaMAX Supplement (Thermo Fisher Scientific; 61965059), 0.01 g L-Cystein (Sigma, Merck; C6852), 200 U papain (Sigma, Merck; P3125), pH 7.4, activated prior to use 30 minutes at 37°C). Tissue was dissociated either with 2 mL or 200 µL pipette in plating medium (DMEM high glucose with GlutaMAX Supplement, 10% FBS (v/v) (Thermo Fisher Scientific; 10270-106), 1% Penicillin/Streptomycin (5000 U/mL) (v/v) (Thermo Fisher Scientific; 15070-063)) for cortical or hippocampal culture, respectively. Dissociated cortical neurons were transferred to a new tube, pelleted at 700 *g* for 5 minutes, while dissociated hippocampal neurons were left for 30 seconds for the clumps to pellet by gravity and transferred the supernatant to the new tube. Both cell suspensions were counted, plated on the PDL coated dishes (25 µg/mL of PDL per well (Sigma, Merck; P6407)) and cultured at 37°C, 5% CO_2. Plating medium was exchanged for culturing medium (9.6 mL Neurobasal (Thermo Fisher Scientific; 21103049), 500 µM GlutaMAX supplement (Thermo Fisher Scientific; 35050061), 1% Penicillin/Streptomycin (5000 U/mL) (v/v), 1 × B27 supplement (Thermo Fisher Scientific; 17504044)) after 3-4 hours.

2.8 | Treatment and collection of primary mouse cortical neurons

BACE1 conditional knockout (BACE1 coKO) neurons were transduced with lentiviruses (Codon-optimized Cre recombinase iCre or control GFP in a pF2U vector; virus purified as described[51]) at day 2 in vitro (DIV). Ubiquitous expression of iCre targets the loxP sites of the floxed BACE1 allele causing excision of exon 2 and subsequent knockout of BACE1 in neurons (Figure S2A). At DIV 4, neurons were washed twice with PBS and finally collected at DIV 6. For the experiments with additional treatment, for both WT and BACE1 coKO, neurons were washed at DIV 5 and 2 µM C3 (BACE1 inhibitor IV, Calbiochem, Merck; 565788), 1 µM DAPT (γ-secretase inhibitor, Sigma, Merck; D5942), or DMSO (control; an equal amount of dissolvent was used to maintain the homogeneity of the experimental conditions) was added and finally collected at DIV 7. Collection was done by lysing the neurons in STET-lysis buffer with protease inhibitor (150 mM NaCl, 50 mM Tris (pH 7.5), 2 mM EDTA, 1% Triton X-100). For electrophysiology, hippocampal neurons between DIV 12 and DIV 15 were grown on a coverslip and pretreated overnight with 2 µM C3 or DMSO.

2.9 | Generation of conditional BACE1 KO (BACE1coKO) mice

For homologous recombination in IDG3.2 cells a EUCOMM based vector was used that contained loxP-flanked exon 2 of the *Bace1* gene. The targeting vector was linearized by *SalI* and used for homologous recombination in embryonic stem (ES) cells (cell line IDG3.2-rosa26 established from (C57BL/6J 3129S6SvEvTac)-F1 blastocysts[52]) as previously described.[53] IDG3.2-rosa26 ES cells were cultured on gelatine-coated cell plates in Standard DMEM containing sodium pyruvate, 15% FCS, 24 µM HEPES, 1 × MEM nonessential amino acids, 120 µM β-mercaptoethanol and leukemia inhibitory factor (LIF) (1.8×10^3 U/mL). ES cells were maintained in a 37°C incubator with humidified atmosphere of 20% O_2 and 5% CO_2. After electroporation, 150 clones were isolated, individually expanded and analyzed for homologous recombination. Eight positive ES cell clones were expanded, and one ES cell clone (Bace-E8) was used for microinjection into BALB/c blastocysts yielding seven chimeric animals. Four of these were backcrossed with C57BL/6J mice and all of them successfully transmitted the conditional *Bace-1* knockout

allele to the germ line. In order to remove the SA-IRESlacz and β-actin promoter-neomycin selectable marker cassettes that are surrounded by flip recombinase target (FRT) sites, the mice were crossed with the flippase (FLP) recombinase containing mice (Tg(ACTFLPe)9205Dym MGI:2448985) (as can be seen in Figure S2). FLP recombination between FRT sites excises the two cassettes to generate the floxed allele of the BACE1 gene exon 2, thus producing the BACE1 coKO mice. Genotypes of mice were verified by ear biopsies DNA polymerase chain reaction (PCR) using primers: 5´-AGGTGTGTGTGGGACTCCAT-3´, 5´-AGGTGTGTGTGGGACTCCAT-3´ and 5´-AGGTGTG TGTGGGACTCCAT-3´ to control the BACE1 FRT conditional knockout, 5`-AGGTGTGTGTGGGACTCCAT-3´, 5´-AGGTGTGTGTGGGACTCCAT-3´forthefloxedBACE1 allele and 5´-CTCGAGGATAACTTGTTATTGC-3´, and 5´-CTAATGTTGTGGGAAATTGGAGC-3´ for the FLP allele.

2.10 | In vitro cleavage assay

The murine peptides (MDGA1—PINPSGPFQIIFEGVRG SGY, CACHD1—KSPYVDDMGAIGDEVITL, Peps4LS GmbH, Heidelberg, Germany) were dissolved in 40% acetonitrile at a concentration of 1 mg/mL. Recombinant BACE1 was preincubated in 50 mM sodium acetate buffer pH 4.4 with or without C3 inhibitor for 15 minutes, at 37°C. An amount of 5 µg of peptides was added to buffer without or with recombinant BACE1, as well as BACE1 and C3 inhibitor. The reaction mixtures were incubated overnight at 37°C. Digested samples were added to the mixture of Sera-Mag SpeedBeads A and Sera-Mag SpeedBeads B (1:1 ratio, Thermo Fisher Scientific, Waltham, MA, USA) and 95% acetonitrile. Samples were centrifuged for 18 minutes at 1000 rpm and room temperature and subsequently washed two times with 100% acetonitrile. Between each wash samples were centrifuged shortly at 16 000 *g* and placed in a magnetic rack. Elution was done with 2% DMSO and the samples were sonicated two times 30 seconds in the water bath. Samples were collected by short centrifugation at 16 000 *g* and separated from the beads using magnetic rack. Peptides were acidified to a final concentration of 1% formic acid for mass spectrometric analysis.

Peptides were separated on an in-house packed 30 cm C18 column (ID: 75 µm, 2.4 µm Reprosil-Pur C18 AQ, Dr Maisch GmbH, Ammerbuch, Germany) using an Easy nLC 1000 (Thermo Fisher Scientific, USA) nanoHPLC system with a binary gradient of water (A) and acetonitrile (B) supplemented with 0.1% formic acid at a flow rate of 250 nL/min (0 minutes, 8% B; 145 minutes, 25% B; 227 minutes, 45% B). The LC was coupled online via a nano electrospray ion source to a Q-Exactive mass spectrometer (Thermo Fisher Scientific, USA). Full MS spectra were acquired at a resolution of 70 000 covering a scan range of 300 to 1400 m/z. The 10 peptide ions with the highest intensities in each scan cycle were chosen for higher energy collisional induced dissociation (min signal: 5E + 4; isolation width: 2 m/z; normalized collision energy: 25%). A dynamic exclusion of 3 seconds was applied for precursor selection to get multiple fragment ion spectra of the cleavage products.

2.11 | Preparation and cultivation of brain slice cultures

Entorhino-hippocampal tissue cultures were prepared at postnatal day 4-5 from C57BL/6J mice of either sex as described previously.[54] Cultivation medium contained 50% (v/v) MEM, 25% (v/v) basal medium eagle, 25% (v/v) heat-inactivated normal horse serum, 25 mM HEPES buffer solution, 0.15% (w/v) bicarbonate, 0.65% (w/v) glucose, 0.1 mg mL-1 streptomycin, 100 U mL-1 penicillin, and 2 mM glutamax. The pH was adjusted to 7.3, and the medium was replaced three times per week. All slice cultures were allowed to mature for at least 18 days in humidified atmosphere with 5% CO2 at 35°C. Tissue cultures were treated for 3 days with 2 µM C3 or DMSO before experimental assessment.

2.12 | Electrophysiological recordings of GABAergic miniature inhibitory postsynaptic currents (mIPSCs) from dissociated mouse primary hippocampal neurons

Mouse primary hippocampal neurons were whole-cell voltage-clamped at −70 mV using EPC10 USB amplifier (HEKA Electronics, Lambrecht/Pfalz, Germany). The acquisition interface was controlled by using Patch master program (HEKA Electronics). In all experiments the following solutions were used: extracellular solution (140 mM NaCl, 2.4 mM KCl, 10 mM Hepes, 10 mM glucose, 4 mM $CaCl_2$, and 4 mM $MgCl_2$, 320 mOsmol/L, pH 7.4); patch-pipette solution (136 mM KCl, 17.8 mM Hepes, 1 mM EGTA, 0.6 mM $MgCl_2$, 4 mM NaATP, 0.3 mM Na_2GTP, 15 mM creatine phosphate, and 5 U/mL phosphocreatine kinase, 310-320 mOsmol/L, pH 7.4). Miniature inhibitory postsynaptic currents (mIPSCs) were recorded in the presence of 300 nM tetrodotoxin (TTX) and 10 µM 2,3-dihydroxy-6-nitro-7-sulfamoyl-benzo (F)quinoxaline (NBQX). Except for TTX (Purchased from Abcam), all chemicals were purchased from Sigma. Data were analyzed using Axograph X version 1.6.5. Further data analysis/visualization was performed by using Graph Pad Prism 7 and Adobe illustrator version CS5.1.

2.13 | Electrophysiological recordings of GABAergic mIPSCs from CA1 pyramidal neurons of entorhino-hippocampal tissue cultures

Whole-cell voltage-clamp recordings were carried out at 35°C. The bath solution contained 126 mM NaCl, 2.5 mM KCl, 26 mM $NaHCO_3$, 1.25 mM NaH_2PO_4, 2 mM $CaCl_2$, 2 mM $MgCl_2$, and 10 mM glucose. Patch pipettes contained 40 mM CsCl, 90 mM K-gluconate, 1.8 mM NaCl, 1.7 mM MgCl2, 3.5 mM KCl, 0.05 mM EGTA, 2 mM ATP-Mg, 0.4 mM GTP-Na2, 10 mM PO-Creatine, and 10 mM HEPES (pH = 7.25 with KOH, 290 mOsm with sucrose) having a tip resistance of 4-6 MΩ. Neurons were recorded at a holding potential of −70 mV in the presence of 0.5 μM TTX, 10 μM CNQX, and 10 μM APV. Series resistance was monitored in 2 minutes intervals, and recordings were discarded if leak current or series resistance changed significantly and/or reached ≥30 MΩ or ≥350 pA, respectively. Data were analyzed using pClamp 10.2 (Axon Instruments) and MiniAnalysis (Synaptosoft) software.

2.14 | Immunofluorescence

For immunofluorescence labeling, COS7 cells were cultured for 48h in DMEM supplemented with 10% fetal calf serum (FCS), 1% Penicillin-Streptomycin (Pen/Strep), and seeded onto PDL-coated glass coverslips. Cells were fixed with 4% paraformaldehyde in 4% sucrose solution for 10 minutes at room temperature and unfixed cells were washed three times with 1x phosphate-buffered saline (PBS). Cells were quenched with 50 mM ammonium chloride for 10 minutes at room temperature and washed three times with 1x PBS. Afterward, cells were incubated with 0.1% Triton X in 1x PBS for 10 minutes and washed three times with 1x PBS. Afterward, cells were blocked in 2% FCS, 2% bovine serum albumin (BSA), 0.2% Fish Gelatin in 1x PBS for 1h at room temperature and incubated over night at 4°C with anti-EEA1 (species: mouse, dilution 1:200), anti-KDEL (species: mouse, dilution 1:200), or anti-Giantin (species: mouse, dilution 1:200) followed by 1h incubation at room temperature with directly fluorophore-coupled anti-GFP-488 (species: rabbit, dilution 1:500, against CACHD1-GFP) and secondary antibody anti-mouse-555 (dilution 1:500) for the three organelle marker primary antibodies. Before and after antibody incubation cells were washed three times with 1x PBS. Nuclei were stained with Hoechst (dilution 1:2000) for 30 minutes at room temperature. Coverslips were mounted in FluorSave (Calbiochem, Merck) onto glass slides and imaged with confocal microscopy using a Leica TCS SP5 Confocal Laser Scanning Microscope (LSM) or Zeiss LSM 510 Axio Observer (Zeiss, Munich, Germany). Pictures were processed with Photoshop (Adobe) or ZEN2 (Zeiss).

2.15 | Deglycosylation assay

Cortical neuronal lysate was treated with endoglycosidase H (Endo H, New England Biolabs, Frankfurt am Main, Germany; P0702), or Peptide-N-Glycosidase (PNGase F, New England Biolabs; P0704) according to the manufacturer's protocol and separated on 8% or 12% SDS-polyacrylamide gel.

2.16 | Retina preparation, histology, and immunohistochemistry

Retinas were dissected at 4 months of age and further processed as described for immunohistology.[55] Ten micrometer thick retinal cross sections were processed for hematoxylin and eosin staining or for immunohistochemistry. Cy3-coupled mouse monoclonal anti-GFAP (Sigma, Merck) was added overnight at a dilution of 1:1000. Nuclei were counterstained with Hoechst 33342. The examined area was determined microscopically by a Leica LSM 510 Meta confocal scan microscope (Zeiss) or a conventional fluorescence microscope (Nikon Eclipse). Quantification of outer nuclear layer thickness was done from images taken from representative central areas from 12 retinal cross sections per biological replicate (n = 3 per genotype).

3 | RESULTS

3.1 | Proteomic analysis of BACE1 KO mouse brains

For BACE1 substrate identification in vivo, we used brains of WT and BACE1 KO mice from P3 when BACE1 protein abundance is high compared to adult mice.[25] BACE1 substrates are transmembrane or glycosylphosphatidylinositol (GPI)-anchored membrane proteins, and inhibition or knockout of BACE1 often leads to an accumulation of BACE1 substrates on the cell surface of BACE1-expressing cells, in particular neurons.[11,14,47] Thus, we scored membrane proteins as in vivo BACE1 substrate candidates if their protein levels in the brain membrane fraction were increased upon knockout of BACE1. The soluble brain fraction was not analyzed, as it does not only contain the extracellular cleavage products of BACE1 substrates, but also the much more abundant cytosolic proteins, which interfere with the detection of the low-abundant BACE1 substrates. In order to accurately monitor even small changes in the membrane proteome of the brain, a spike-in of mouse brain tissue with Stable Isotope Labeling by Amino acids (SILA) combined with a quantitative proteomic workflow was used (Figure 1A). Brains from commercially available SILA ^{13}C lysine-labeled P3 WT mice were used as reference brain tissue,

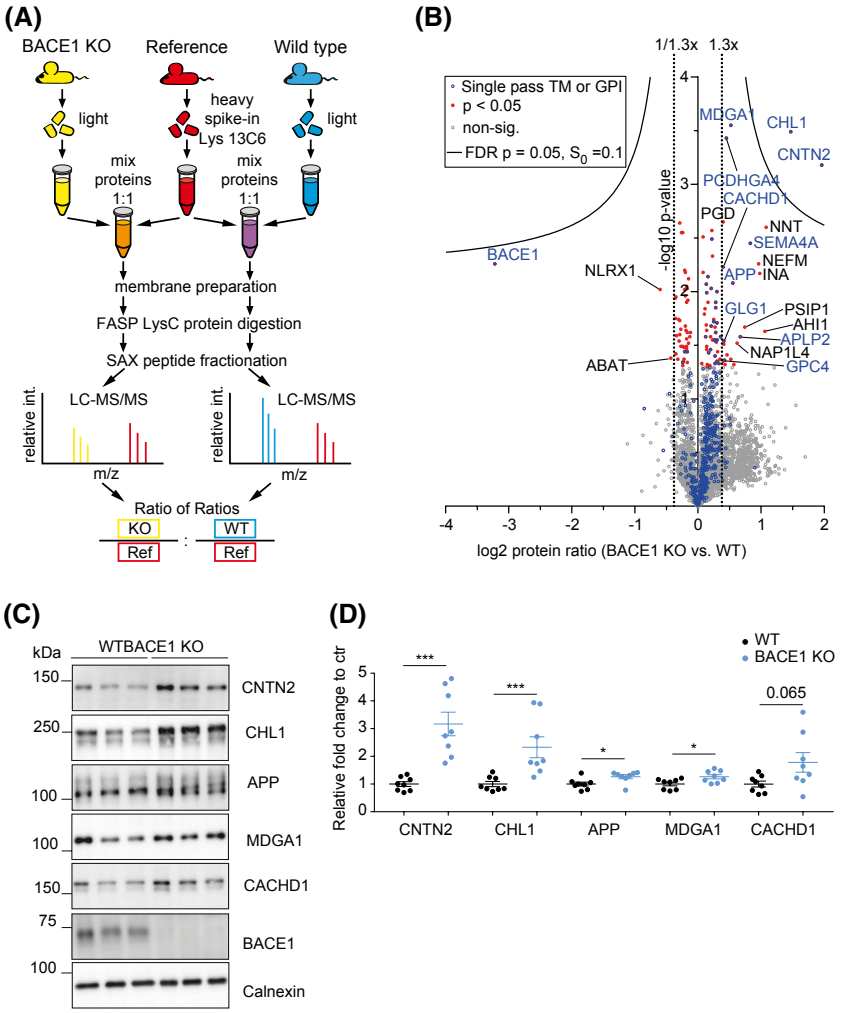

FIGURE 1 BACE1 substrate identification in vivo. A, Proteomic workflow of the Stable Isotope Labeling by Amino acids (SILA) spike-in approach. Isotopically heavy ($^{13}C_6$) labeled mouse brain tissue was combined with unlabeled (light) mouse brain tissue from wild-type (WT) or BACE1 KO mice. WT and BACE1 KO mice were littermates. B, Volcano plot of membrane fractions of BACE1 KO and WT mouse brains. The negative log10 transformed *P* value (*y*-axis) is plotted against the mean protein log2 fold change (*x*-axis) between BACE1 KO and WT samples. Single-span transmembrane proteins and GPI-anchored proteins are colored in blue. The hyperbolic curves represent a permutation-based FDR correction for multiple hypotheses. Proteins above the FDR curve remain significantly changed after FDR correction. C, Western blot analysis of the membrane preparation of WT, and BACE1 KO mouse brains at P3 shows accumulation of full-length CNTN2, CHL1, APP, MDGA1, and CACHD1. D, Statistical analysis was performed with n = 8 biological replicates using Mann-Whitney U test with the significance criteria of $P < .05$. All proteins accumulate significantly, except for CACHD1 that shows a nonsignificant trend to an increase. Graphs are presented with mean ± SEM

where all proteins contain lysines labeled with six heavy ^{13}C isotopes. These reference brains were mixed (spike-in approach) with brain tissue from our unlabeled mice, either WT or BACE1 KO, and further processed for mass spectrometric analysis, including the LysC digestion. The protease LysC cleaves proteins at the C-term of lysines. Thus, all peptides derived from the SILA spike-in possess at least one heavy labeled lysine, which introduces a mass shift of 6 Da in comparison to the peptides originating from unlabeled WT or BACE1 KO samples. Eventually, a duplet of peptide signals with unlabeled and heavy labeled lysines is detected by mass spectrometry and is used for relative quantification of proteins (Figure 1A). This method allows a normalization of all peptide intensities from WT or BACE1 KO samples to the corresponding heavy reference peptides of the spike-in, yielding the ratios WT/reference and BACE1 KO/reference for relative protein quantification. The MS data analysis software Maxquant reports heavy to light protein ratios. For relative quantification, ratios were inverted to obtain WT (light) and BACE1 KO (light) to reference (heavy) ratios which allowed to calculate average KO to WT protein ratios and to perform a statistical evaluation of protein abundance changes. The normalization of protein intensities to the spike-in minimizes quantification inaccuracies due to membrane preparations, extensive peptide fractionation, and LC-MS/MS performance over several days of measurement.

Membrane fractions from three biological replicates (WT and BACE1 KO brains) were proteomically analyzed. Overall, 2932 proteins were relatively quantified in at least two biological replicates. This included proteins that are annotated in Uniprot as integral membrane proteins or membrane-associated proteins, but also soluble proteins which are likely to bind to integral or membrane-associated proteins. BACE1 substrates are usually single-span transmembrane proteins with type 1 (TM1) topology or GPI-anchored proteins, but can also have a TM2 topology. Here, we have relatively quantified 1064 transmembrane or GPI-anchored proteins, which contain 464 single-pass or GPI-anchored proteins (Data S1).

The membrane proteins were scored as BACE1 substrate candidates if their level increased by at least 30% (vertical dotted line in the volcano plot in Figure 1) and if the change reached a significance of less than 0.05 using a two sample Student's *t* test (corresponding to a value higher than 1.3 on the logarithmic y-axis, Figure 1B). This led to 10 transmembrane or GPI-anchored proteins being identified as potential BACE1 substrates, including the known BACE1 substrates APP[17] (1.47-fold increase), APLP2[56,57] (1.59-fold), CNTN2[11] (3.90-fold), and CHL1[11,30] (2.76-fold), which validated our proteomic screening approach. Furthermore, we observed an accumulation for the transmembrane type I protein CACHD1 (1.32-fold), which is a suggested BACE1 substrate candidate,[11,13] and the GPI-anchored protein MDGA1 (MAM domain-containing glycosylphosphatidylinositol anchor protein 1) (1.44-fold), which is a novel BACE1 substrate candidate. Additionally, we found increased protein levels of the transmembrane or GPI-anchored proteins PCDHGA4 (1.37-fold) and GLG1 (1.33-fold), which are suggested BACE1 substrate candidates,[11-14] and of SEMA4A (1.78-fold), and GPC4 (1.34-fold), which are new potential BACE1 substrates. Thus, the proteomic analysis identified known BACE1 substrates or candidates as well as new BACE1 substrate candidates.

In addition, thirteen soluble or mitochondrial proteins were found to be enriched in the KO samples. Two mitochondrial multi-pass transmembrane proteins, NNT and SLC25A31, were found with an increased abundance. Moreover, 10 soluble proteins, namely NEFM, INA, PSIP1, AHI1, NAP1L4, VIM, GNAL, MYL6, ATIC, and GPI, were detected with a higher abundance in the KO samples. Because so far known BACE1 substrates are exclusively membrane proteins and BACE1 is localized in the TGN and endosomes, it is likely that the identified soluble and mitochondrial proteins do not constitute BACE1 substrates but were enriched as an indirect consequence of BACE1-deficiency. Three proteins were reduced in the BACE1 KO brains (NLRX1, ABAT, and BACE1). The reduction of BACE1 in the BACE1 KO brains was expected. The low amount of still detected BACE1 in the KO brains is most likely the result of a small carry-over effect between KO and WT LC-MS/MS runs.

Next, we validated the mass spectrometric measurements using immunoblots as a different method. Similar to the proteomic experiments, membrane fractions were generated from BACE1 KO and WT mouse brains. In agreement with the proteomic mouse brain data, the full-length levels of both MDGA1 and CACHD1 showed a mild increase in the BACE1 KO membrane fractions (Figure 1C,D), while the levels of the soluble MDGA1 and CACHD1 ectodomains in the soluble brain fraction were below the detection limit, presumably, because this soluble fraction does not only contain the extracellular cleavage products of BACE1 substrates, but also the much more abundant cytosolic proteins. Full-length levels were also increased for the two established BACE1 substrates CNTN2 and CHL1 (Figure 1C,D).

3.2 | Validation of MDGA1 and CACHD1 as BACE1 substrates

Next, we validated whether CACHD1 and MDGA1 are indeed substrates of BACE1 or if their accumulation is a consequence of secondary effects due to BACE1 deletion. To this aim, we monitored whether BACE1 inhibition abolishes the occurrence of a cleavage product of the substrates. CACHD1 was chosen as it had the smallest fold change (1.32) of the substrate candidates and was previously identified as a potential substrate in other proteomic studies,[11,13] but was not yet validated. MDGA1 was chosen because it had the best significance value of the substrate candidates and because it is a novel BACE1 substrate candidate.

Both MDGA1 and CACHD1 are membrane proteins with a topology that potentially allows cleavage by BACE1. MDGA1 is a GPI-anchored protein and has six Ig-like, a fibronectin type-III and a MAM domain (Figure 2A). In contrast, CACHD1 is a single-pass type 1 membrane protein with two Cache and one VWFA domain (Figure 3A). As it was not yet studied molecularly at the beginning of our study, we tagged CACHD1 with a C-terminal GFP-tag and found that it indeed localized to cellular membranes in transfected COS7 cells, as expected for a transmembrane protein (Figure S1). We observed a localization to the plasma membrane and the Golgi and partly to the endoplasmic reticulum and endosomes, in agreement with two very recently published studies on CACHD1.[58,59]

Validation of MDGA1 and CACHD1 as BACE1 substrates was done using primary murine neurons, where BACE1 was either pharmacologically or genetically inactivated. For the pharmacological inhibition, neurons were treated with a BACE1 inhibitor (BI, either BACE1 inhibitor C3[60] - also known as BACE1 inhibitor IV - or LY2886721[61]) or DMSO as a control. The non-cleaved, full-length proteins MDGA1 and CACHD1 were detected by immunoblots in the cell lysate (Figures 2B and 3B), where both

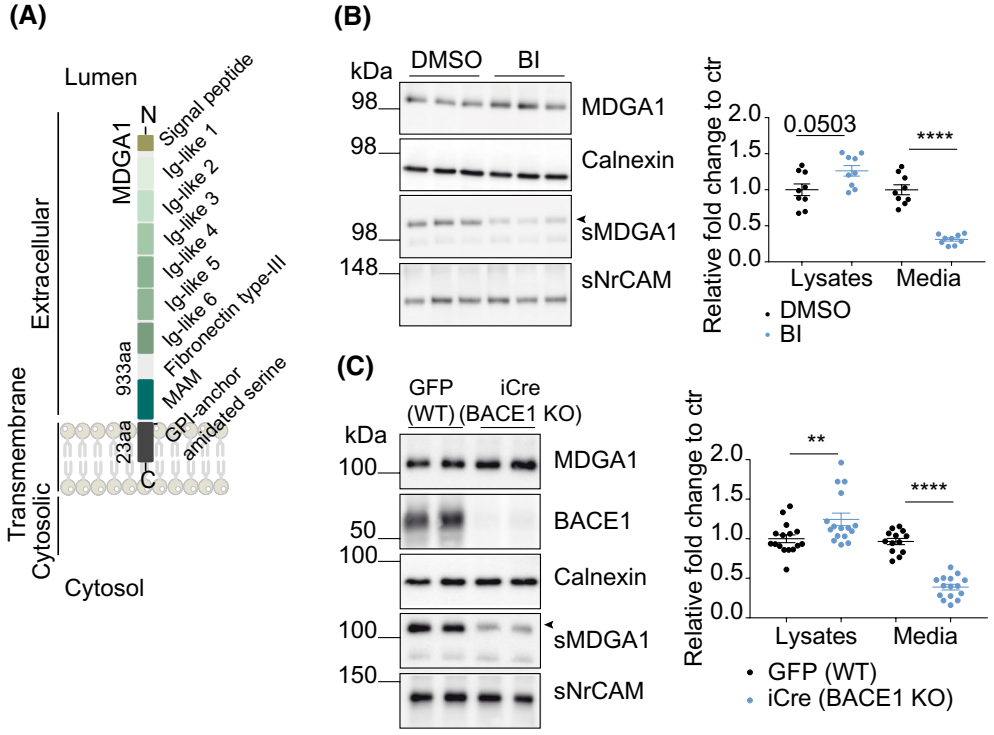

FIGURE 2 Validation of MDGA1 as BACE1 substrate in primary neurons. A, Schematic domain structure representation of MDGA1. The number of amino acids (aa) in each domain is indicated. B, Primary cortical neurons from WT mice were treated with BACE1 inhibitor (BI) or DMSO as a control. MDGA1 full-length protein (MDGA1) was mildly increased in total lysates, whereas its cleaved, soluble ectodomain (sMDGA1) in the conditioned medium was reduced upon BACE1 inhibition (labeled with arrowhead). Data were analyzed using Mann-Whitney U test with the significance criteria of $P < .05$ and are shown relative to the control (ctr) condition with DMSO. C, BACE1 coKO neurons were treated with iCre virus to induce BACE1 KO or with GFP virus to maintain BACE1 expression. MDGA1 accumulated upon BACE1 deletion in total cell lysates of BACE1 conditional knockout neurons, whereas the soluble ectodomain of MDGA1 (sMDGA1) was significantly reduced in the conditioned medium applying Mann-Whitney U test with the significance criteria of $P < .05$. Graphs are presented with mean ± SEM

proteins showed an about 1.2-fold enrichment upon BACE1 inhibition, in agreement with the proteomic data (Figure 1). The BACE1-cleaved soluble ectodomain of MDGA1 (sMDGA1) was detected in the conditioned medium and was reduced to 30% upon BACE1 inhibition (Figure 2B), in line with MDGA1 being a new BACE1 substrate and no longer being efficiently processed upon BACE1 inhibition. For CACHD1, no antibody was available for detection of the endogenous BACE1-cleaved soluble ectodomain (sCACHD1). Thus, we detected the other fragment arising from BACE1 cleavage, namely the CACHD1 C-terminal fragment (CTF), which was detected in the neuronal cell lysate (Figure 3B). As CACHD1 is a type I membrane protein, its CTF may potentially be further cleaved by γ-secretase after the initial BACE1 cleavage, which would be similar to APP.[62-64] In fact, similar to what is known for APP we detected the CACHD1 CTF only after pharmacological inhibition of γ-secretase with DAPT,[65] demonstrating that CACHD1 is also a substrate for γ-secretase. Importantly, the CACHD1 CTF was no longer seen upon additional inhibition of BACE1, revealing that CACHD1 is indeed a substrate for BACE1 (Figure 3B).

Next, genetic inactivation of BACE1 was used and the full-length proteins and their cleavage products were again detected by immunoblots. We generated conditional BACE1 KO mice (BACE1 coKO) (Figure S2) and prepared primary cortical neurons that were treated with control (GFP) virus (keeping BACE1 expression) or iCre virus (inducing BACE1 KO) at day 2 in vitro (DIV 2). Cell lysates and conditioned media were collected at DIV 6 to DIV 7 to provide enough time for the deletion of BACE1, which was successfully achieved (immunoblot in Figures 2C and 3C). For CACHD1, the γ-secretase inhibitor DAPT was additionally applied at DIV 5 to detect the CACHD1 CTF. Similar to BACE1 inhibitor-treated neurons, MDGA1 full-length protein was significantly increased in total cell lysates, accompanied by a strong reduction of its shed ectodomain in the conditioned media upon BACE1 deletion (Figure 2C). Likewise, full-length CACHD1 accumulated in the total cell lysates, while the levels of the CACHD1 CTF were clearly decreased in the iCre infected BACE1 coKO neurons (Figure 3C).

In order to not only detect the CACHD1 CTF, but also the other cleavage products arising from BACE1 cleavage—sCACHD1—we overexpressed CACHD1 with an

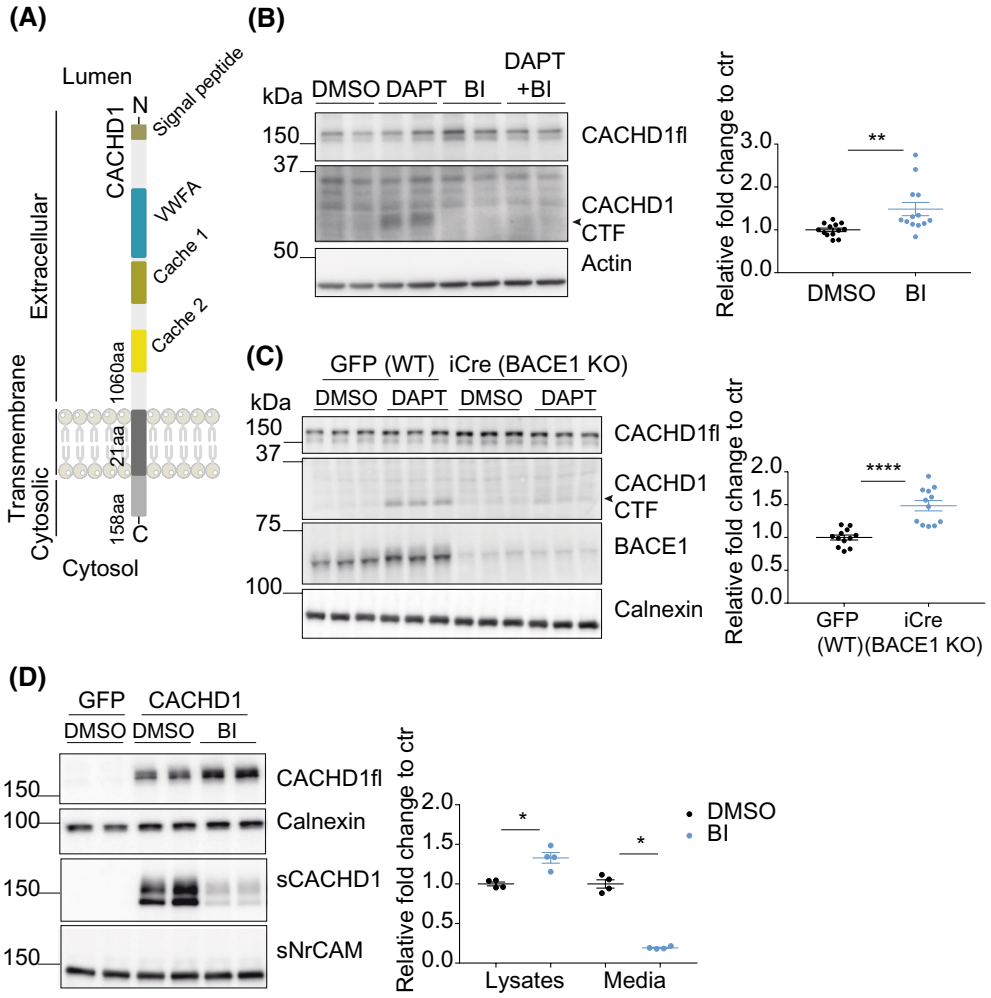

FIGURE 3 Validation of CACHD1 as BACE1 substrate in primary neurons. A, Schematic domain structure representation of CACHD1. The number of amino acids (aa) in each domain is indicated. B, Validation of CACHD1 in WT cortical neurons, treated with γ-secretase inhibitor (DAPT), BACE inhibitor (BI), a combination of DAPT and BI or solvent control (DMSO). CACHD1 full-length (CACHD1 fl) protein was significantly accumulated in the cell lysate upon BACE1 inhibition using Mann-Whitney U test with the significance criteria of $P < .05$. The short-lived CACHD1 C-terminal fragment (CACHD1 CTF, labeled with arrowhead) was detected in the lysate upon inhibition of γ-secretase with the inhibitor DAPT. Its generation was blocked, when BACE1 was additionally inhibited with BI. C, BACE1 coKO neurons were treated with iCre or GFP control lentivirus to induce BACE1 KO or WT condition, respectively. CACHD1 fl significantly accumulated upon BACE1 deletion in total cell lysates applying Mann-Whitney U test with the P value less than .05. CACHD1 CTF was detected in the lysate with DAPT treatment. Its generation was blocked, when BACE1 was knocked-out. D, To detect the soluble ectodomain of CACHD1 (sCACHD1), which is released from cells after BACE1 cleavage, primary cortical neurons were transduced with a CACHD1 lentivirus construct having an N-terminal HA- and a C-terminal FLAG epitope tag. In addition, neurons were treated with BACE1 inhibitor (BI) or DMSO as a control. Upon BACE1 inhibition CACHD1 fl protein significantly accumulated in the neuronal lysate (detected with anti-CACHD1 antibody), whereas release of its ectodomain (sCACHD1, detected with anti-HA antibody) into the conditioned medium was largely abolished. Mann-Whitney U test was used to determine significance criteria of $P < .05$. All graphs are presented with mean ± SEM

N-terminal HA-tag in primary cortical neurons using a lentivirus system. As expected, full-length CACHD1 accumulated in total lysates whereas its shed ectodomain (sCACHD1, detected with an anti-HA antibody) was almost abolished in conditioned media upon inhibition of the endogenous neuronal BACE1 (Figure 3D). Taken together, the pharmacological and genetic experiments as well as the proteomic experiments in Figure 1 demonstrate that MDGA1 and CACHD1 are BACE1 substrates both in vitro and in vivo.

3.3 | Determination of cleavage sites in MDGA1 and CACHD1

Sheddases often cleave their substrates within the ectodomain at a short distance from the beginning of the transmembrane domain in the so-called juxtamembrane domain. This is also seen for different BACE1 substrates, such as APP,[17] SEZ6L,[11] and SEZ6.[47] To determine the cleavage sites of BACE1 within the juxtamembrane domains of MDGA1 and CACHD1, an in vitro assay was performed.

We incubated peptides of the juxtamembrane regions of MDGA1 (PINPSGPFQIIFEGVRGSGY) and CACHD1 (KSPYVDDMGAIGDEVITL) with recombinant BACE1, without BACE1 or with BACE1 in the presence of the BACE1 inhibitor C3 (Figure 4). Separation of the peptide and its cleaved fragments was done by nano liquid chromatography followed by LC-MS/MS analysis. For both peptides, BACE1-dependent cleavage products were identified which were not detected or strongly reduced when BACE1 was inhibited or absent. The PINPSGPFQIIF peptide representing the N-terminal cleavage product of the MDGA1 peptide was detected upon BACE1 application which was strongly reduced upon inhibition with C3 (Figure 4A). For CACHD1, we have identified the N-terminal

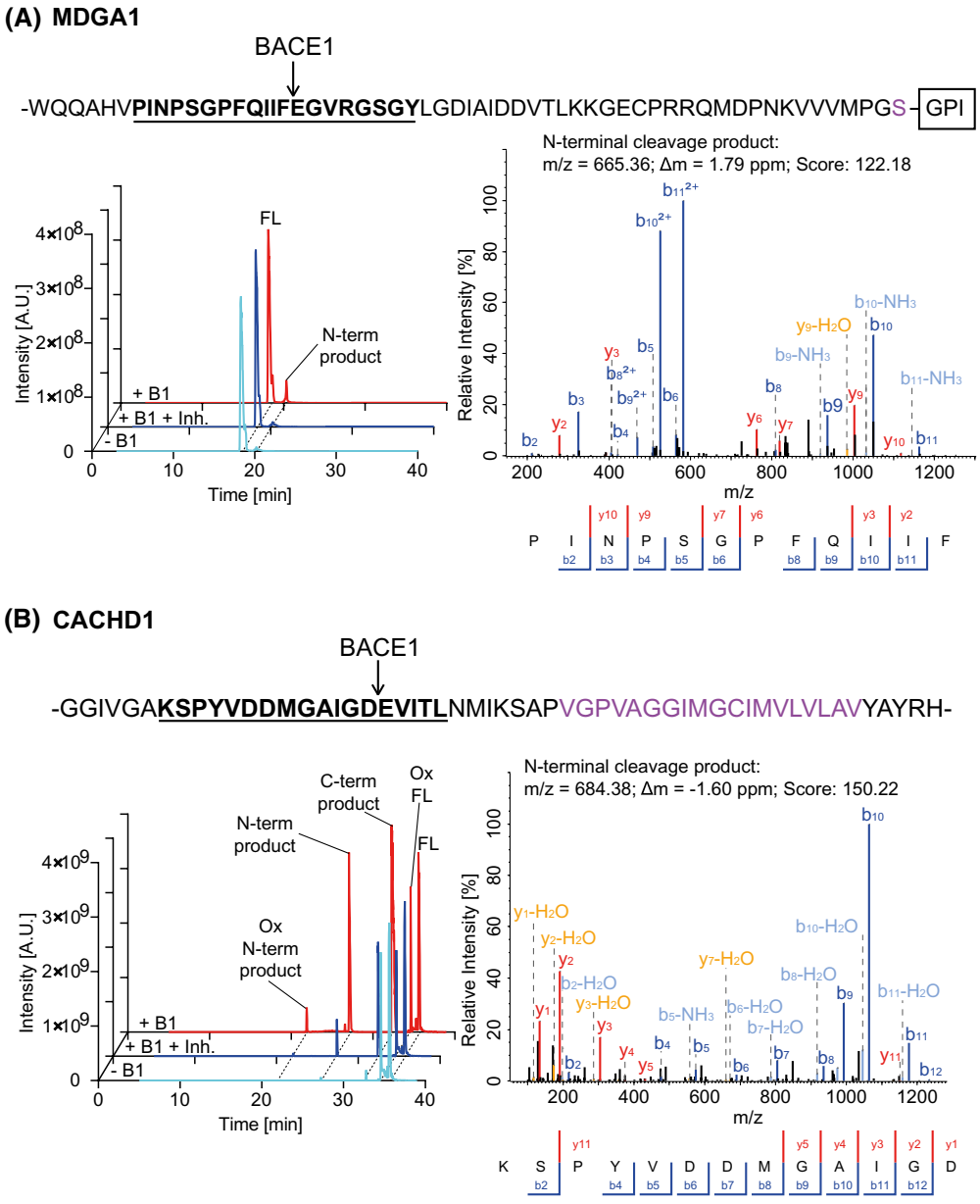

FIGURE 4 BACE1 cleavage site determination of MDGA1 (A) and CACHD1 (B). In the sequence views, peptides close to the cell membrane that were chosen for an in-vitro cleavage assay are indicated in bold black letters. The GPI-anchor amidated serine of MDGA1 and the transmembrane region of CACHD1 are highlighted with bold purple letters. The two peptides were incubated with recombinant BACE1, with BACE1 and its inhibitor C3, or without BACE1. The corresponding extracted ion chromatograms of the full-length peptides (FL) as well as the identified cleavage products are presented in a stacked view (red: BACE1, blue: BACE1 + C3 inhibitor, cyan: without BACE1). For MDGA1, an N-terminal cleavage product was detected which was strongly reduced upon BACE1 inhibition or in its absence. Similarly, for CACHD1, an N-terminal and a C-terminal cleavage product were identified, as well as the oxidized (Ox) N-terminal product that all showed a strong intensity decrease when BACE1 was inhibited by C3 whereas almost no signal was detected if BACE1 was absent. Full-length protein was also detected in its oxidized form (Ox FL). The N-terminal cleavage products were identified by fragment ion spectra with high mass accuracy and high ion scores. The determined cleavage sites are indicated in the sequence views

cleavage product KSPYVDDMGAIGD as well as the C-terminal cleavage product EVITL, which was strongly reduced when BACE1 was inhibited (Figure 4B). For both MDGA1 and CACHD1 the cleavage site has the acidic amino acid glutamate (E) at the P1′ site (the amino acid C-terminal to the cleavage site). A glutamate at the same position is also found in another BACE1 substrate, seizure 6-like protein (SEZ6L), and the equally acidic amino acid aspartate is found in the additional BACE1 substrates APP and SEZ6.[11,47,66] Thus at the P1' site the newly identified cleavage sites are in agreement with cleavage sites identified in other substrates. For the amino acid at the P1 site (directly N-terminal to the cleavage site) MDGA1 has phenylalanine, which is hydrophobic, similar to leucine that is found at this position in other BACE1 substrates, such as SEZ6 and the Swedish mutant of APP.[47,66] For CACHD1 the P1 amino acid is aspartate, which has not been observed at this position in other BACE1 substrates. However, for most BACE1 substrates the cleavage sites have not yet been identified and an in vitro BACE1 cleavage study using decameric peptides revealed that BACE1 in general has a loose sequence specificity,[66] so that there is no common cleavage signature motif for this protease. In conclusion, these data identify the BACE1 cleavage site of MDGA1 between phenylalanine893 and glutamate894 and CACHD1 between aspartate1097 and glutamate1098 (Figure 4).

3.4 | BACE inhibition affects inhibitory synaptic transmission

Among other phenotypes, BACE1 KO mice present with reduced inhibitory transmission in the hippocampus, but excitatory transmission is affected as well.[29,67] While it is not yet exactly clear which BACE1 substrates contribute to these phenotypes, it is interesting that several BACE1 substrates and substrate candidates have a function in synaptic transmission. This includes SEZ6,[27,28] Neuroligin-2 (NLGN2),[68] and our newly identified BACE1 substrate MDGA1.[69] Notably NLGN2 and MDGA1 bind each other at inhibitory synapses but have opposite effects on inhibitory synapse formation and maintenance. It is not known whether the mildly increased levels of MDGA1 observed in BACE1 KO brains would be sufficient to reduce inhibitory synapse formation and function. Given that one phenotype, retina degeneration, was previously reported in only one BACE1 KO mouse line,[70] but was not obviously seen in the BACE1 KO mouse line used here (Figures S3 and S4), we used a pharmacological approach to test whether the reported reduction in inhibitory synaptic transmission previously reported for one BACE1 KO mouse line[67] is also seen with pharmacological BACE1 inhibition. To test the effects of BACE1 inhibition on mIPSCs, we used primary hippocampal WT mouse neurons (Figure 5A-C) as well as organotypic hippocampal tissue cultures containing the entorhinal cortex and hippocampus from WT mice (Figure 5D-F) and blocked BACE1 with the inhibitor C3. In agreement with the previous BACE1 KO study,[67] inhibition of BACE1 reduced the frequency, but not the amplitude of mIPSCs. This demonstrates that the role of BACE1 on inhibitory currents is independent of the mouse line used and is preserved both in dissociated hippocampal neurons as well as in neurons from organotypic cultures with intact hippocampal connectivity.

4 | DISCUSSION

The protease BACE1 has major functions in the nervous systems as revealed by studies of BACE1-deficient mice.[39] Because the function of a protease is determined by its substrates, it is essential to identify BACE1 substrates, their respective function and how these are modulated by BACE1. While this was previously achieved for some BACE1 substrates, the functional consequence of the BACE1 cleavage of other substrates is not yet established. Moreover, numerous additional membrane proteins were identified as BACE1 substrate candidates, mostly by proteomic studies, but not yet validated. With proteomic and biochemical analysis of mouse brains and primary neurons, our study adds the two membrane proteins MDGA1 and CACHD1 to the growing list of BACE1 substrates that are validated in vitro and in vivo.

MDGA1 has diverse functions, for example as a cell adhesion protein in migration and positioning of a subset of neurons in the cortex during mouse development.[71,72] Another function that is well understood at the molecular and structural level, is its role as a negative regulator of trans-synaptic cell adhesion across inhibitory synapses.[73-75] MDGA1 selectively binds neuroligin-2 (NLGN2) in cis at the postsynapse and thereby prevents NLGN2 from establishing firm trans-synaptic interactions with a presynaptic neurexin. Thus, MDGA1 and NLGN2 have opposite functions in inhibitory synapse formation. As a consequence, overexpression of MDGA1 reduced the number of inhibitory synapses in cultured hippocampal neurons, resulting in reduced frequency of mIPSCs, with the amplitude of the currents not being affected.[73,74] Conversely, MDGA1-deficiency in mice induced increased inhibitory synapse formation in the hippocampus and increased mIPSC frequency with no change of the amplitude.[73-75] This established function of MDGA1 is attributed to full-length MDGA1, but the crystal structures of MDGA1 bound to NLGN2 were obtained with the recombinant, soluble ectodomains of both proteins.[76,77] Thus, it appears possible that not only full-length, but also the BACE1-cleaved soluble MDGA1 may bind to NLGN2 in vivo and affect the binding of NLGN2 to neurexins. Interestingly, NLGN2 itself has

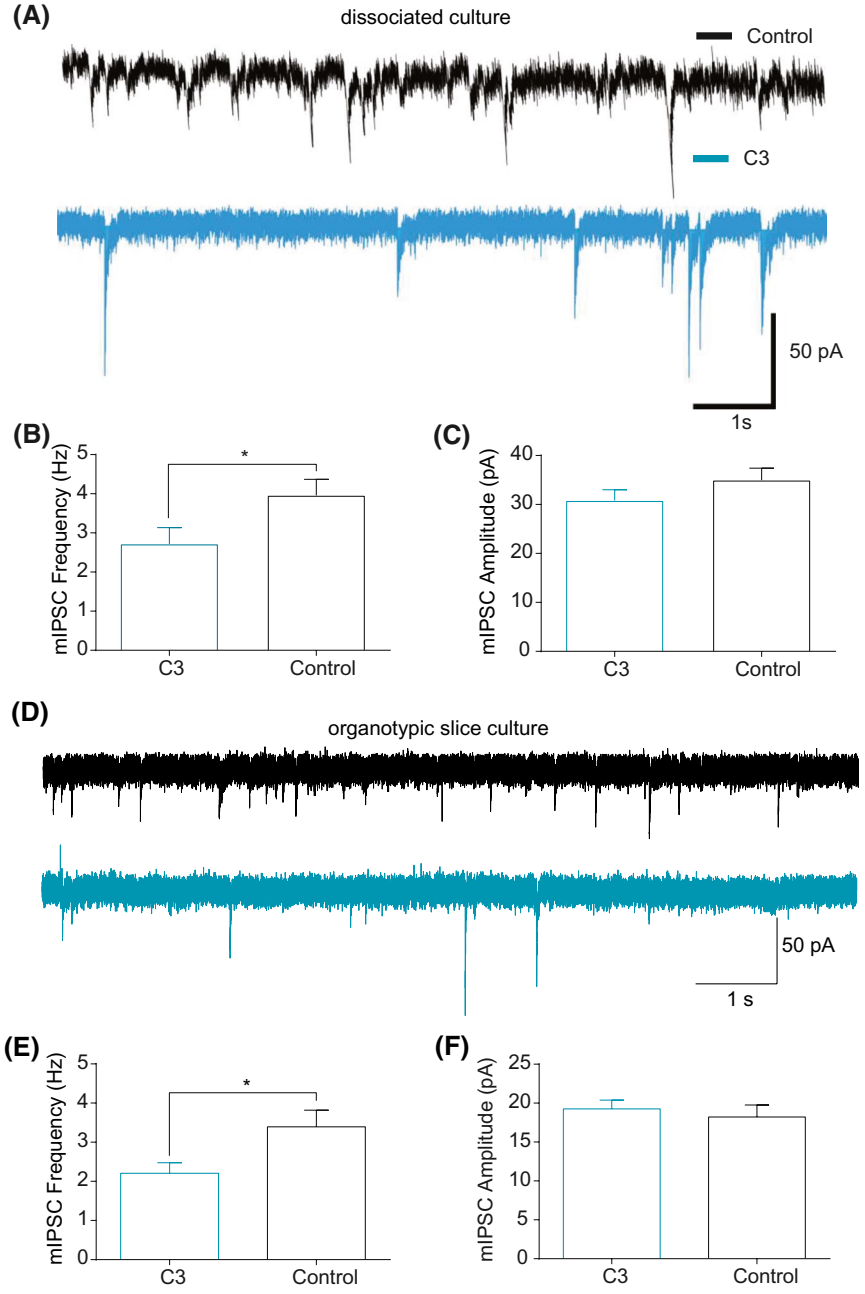

FIGURE 5 Pharmacological inhibition of BACE1 decreases the frequency of miniature inhibitory postsynaptic currents in dissociated cultured hippocampal neurons and in hippocampal neurons from organotypic hippocampal slices. A and D, Representative traces of mIPSCs from neurons pretreated with DMSO (control) in black and BACE inhibitor (C3) in blue, in dissociated cultured hippocampal neurons (A) and in CA1 pyramidal neurons from entorhino-hippocampal slice cultures (D), respectively. B, E and C, F, Mean mIPSC frequencies and mIPSC amplitude of the neurons pretreated with BACE inhibitor (C3, blue) and (DMSO, black), respectively. Note the significant decrease in the mIPSC frequencies of C3 treated neurons (B, E). Data in (B, C) were obtained from n = 26-28 neurons in 3-4 independent experiments. Data in (E, F) were obtained from n = 27 neurons and their statistical analysis were performed using unpaired *t* test with the significance criteria of $P < .05$. Graphs are presented with mean ± SEM

been suggested as a BACE1 substrate candidate, but not yet been validated.[11] Given the potentially multiple interactions between MDGA1 and NLGN2, it remains unclear how BACE1 affects the opposite functions of MDGA1 and NLGN2 in inhibitory synaptic transmission. On the one hand, it may be speculated that the mildly increased levels of MDGA1 observed in BACE1 KO brains may be sufficient to reduce inhibitory synapse formation and function. This would be consistent with the reduced inhibitory postsynaptic currents upon BACE1 inhibition in hippocampal neurons from dissociated cultures as well as organotypic hippocampal slices, as observed here and previously in acute hippocampal slices from BACE1 KOs.[67] On the other hand, though, the levels of the substrate candidate NLGN2 would be expected to be increased as well and may sequester the increased MDGA1 levels, thus not resulting in a change in inhibitory synapse formation. Yet, other BACE1 substrates, such as SEZ6, voltage-gated sodium channels, Jagged, and Nrg1, also affect directly or indirectly synaptic transmission.[25-28,32,78,79] Thus, synaptic alterations in BACE1-deficent mice may not be attributed easily to individual substrates, but may reflect complex changes in the function of multiple substrates.

The second validated BACE1 substrate in our study is CACHD1. Two very recent studies provided the first biochemical and functional characterization of CACHD1, using overexpression of CACHD1 in kidney and neuroblastoma cell lines and in hippocampal neurons. They demonstrate

that CACHD1 closely interacts with voltage-gated calcium channels of the N-type[58] and T-type[59] at the cell surface and enhances the densities of their calcium currents. Both studies suggest that CACHD1 may be acting as a new auxiliary subunit of voltage-activated N- and T-type calcium channels. This is reminiscent of the known function of a CACHD1 homolog, α2δ, a known auxiliary subunit of Cav1 and Cav2 channels.[80] Despite functional similarities, CACHD1 and α2δ also have distinct features and one of them involves their proteolytic processing. After biosynthesis, the GPI-anchored protein α2δ undergoes proteolytic maturation, where an as yet unknown protease cleaves within the ectodomain of α2δ, yielding the α2 and the δ subunit which remain linked as a heterodimer through disulfide bridges.[81,82] Similar proteolytic heterodimer formations with or without disulfide bridges are known for other membrane proteins, such as Notch,[83] NrCAM,[84] and the insulin receptor.[85,86] While evidence for proteolytic processing of CACHD1 was not reported in the two recent functional studies,[58,59] our study demonstrates CACHD1 cleavage by BACE1. Compared to α2δ, where the proteolytic cleavage site in the ectodomain is more than 100 amino acids away from the transmembrane domain (according to Uniprot), the cleavage site in CACHD1 was found to be at a distance of only 12 amino acids from the membrane. Given that the soluble CACHD1 ectodomain arising through BACE1 cleavage is found in the conditioned medium of cultured cell lines and primary neurons (this study and[11]), it appears unlikely that it forms a heterodimer with the CACHD1 CTF in a manner comparable to α2δ. Instead, BACE1 cleavage of CACHD1 looks like a typical example of ectodomain shedding of membrane proteins,[1] which may serve different molecular functions, such as the termination of the function of a full-length membrane protein. Thus, it appears possible that BACE1 cleavage is a mechanism to control CACHD1's function in calcium signaling and synaptic transmission.[58,59]

Yet, other functional scenarios also appear possible for the BACE1 cleavage of CACHD1. The BACE1-cleaved sCACHD1 ectodomain may have an as yet unknown physiological function, similar to what was reported for other membrane proteins, such as death receptor 6 (DR6), where the full-length membrane protein acts as a receptor controlling cell death, but the cleaved ectodomain acts as a cytokine suppressing myelination.[87] Importantly, similar to numerous other type I membrane proteins,[88] we found that CACHD1 is not only subject to ectodomain shedding by BACE1, but also to subsequent cleavage by γ-secretase, which generates additional cleavage products, such as the intracellular domain that may itself have a role in signal transduction and gene regulation, as it is established for the Notch receptor.[89] Whether γ-secretase cleavage of CACHD1 also leads to functional cleavage products or is merely a way to degrade the membrane-bound CACHD1 CTF, remains to be determined.

Another outcome of our study relates to proteomic strategies for identifying BACE1 substrates. Full-length protein levels of MDGA1 and CACHD1 were only mildly increased (less than 30%) in the cell lysate or the brain membrane fraction upon BACE1-deficiency. In contrast, in the conditioned medium the reduction of the cleaved, secreted ectodomain was much more prominent with a 60%-70% decrease for MDGA1 and an 80% decrease for CACHD1. Similar observations were made in our initial proteomic mouse brain analysis, where most detected BACE1 substrates, such as APP or APLP2, showed a modest increase of less than twofold of their full-length protein levels in the BACE1 KO brain membrane fraction, with only two proteins (CHL1, contactin-2) showing an increase larger than twofold. Likewise, a previous study determining changes of the neuronal surface membrane proteome upon pharmacological BACE1 inhibition reported a less than twofold increase for most BACE1 substrates,[90] demonstrating that the effect size of the enrichment of full-length BACE1 substrates in the lysate or membrane is relatively small upon BACE1 inhibition or deficiency. In contrast, previous proteomic studies analyzing changes of the cleaved ectodomains of BACE1 substrates in the conditioned medium of cells or in the cerebrospinal fluid reported larger fold changes,[11,12,15,47] similar to our observation here with MDGA1 and CACHD1. Thus, for potential future BACE1 substrate identification screens, it appears preferable to measure the larger changes in the levels of the cleaved substrate ectodomains rather than the smaller changes of the full-length proteins in the lysates or membranes.

Taken together, our study adds MDGA1 and CACHD1 to the growing list of validated BACE1 substrates. This has implications for both basic and disease-related neuroscience. Given that MDGA1 and CACHD1 have fundamental functions in inhibitory synapse formation and voltage-gated calcium channel signaling, respectively, it appears possible that BACE1 modulates both processes, but its exact role needs to be elucidated in more detail. Interestingly, MDGA1 has been genetically linked to psychiatric diseases, such as schizophrenia and bipolar disorder.[91,92] Notably, several psychiatric side effects, such as suicidal ideation, anxiety, psychotic symptoms, and depression were also reported for a small percentage of individuals treated with BACE1-targeted inhibitors in phase 3 trials of AD.[21,22] Moreover, BACE1-deficient mice show several defects in the nervous system, such as epileptic seizures and schizophrenic symptoms. While it is not yet known which in vivo BACE1 substrates contribute to what extent to the observed phenotypes, the continued identification and validation of BACE1 substrates is an important step toward a comprehensive understanding of in vivo BACE1 functions at the molecular level and of side effects occurring in BACE1 clinical trials.

ACKNOWLEDGMENTS

We thank Katrin Moschke, Anna Berghofer, and Olena Yefremova for excellent technical help and Christos Galanis, Julia Muellerleile, and Charlotte Nolte-Uhl for help with patch-clamp experiments and data analysis. This work was supported by the Deutsche Forschungsgemeinschaft (German Research Foundation) within the framework of the Munich Cluster for Systems Neurology (EXC 2145 SyNergy, project ID 390857198), (JE 528/6-1) and the collaborative research unit FOR2290 as well as the BMBF project CLINSPECT-M, the Swedish Society of Medicine, the Swedish Society for Medical Research and the Alzheimer Forschung Initiative e.V. (15038).

CONFLICT OF INTEREST

The authors declare no conflicts of interest.

AUTHOR CONTRIBUTIONS

S.F. Lichtenthaler designed research; J. Rudan Njavro, J. Klotz, B. Dislich, J. Wanngren, J. Herber, and S.A. Müller performed research; J. Rudan Njavro, P.-H. Kuhn, and R. Feederle generated antibodies; M. Conrad and W. Wurst generated the BACE1 conditional knockout mouse; MD Shmueli contributed to performing the cleavage assay of CACHD1; R. Kumar and T. Koeglsperger performed electrophysiological recordings of primary hippocampal neurons; A. Vlachos and P. Jedlicka performed electrophysiological recordings of organotypic hippocampal tissue cultures. S. Michalakis performed experiments in retina; S.A. Müller and J. Rudan Njavro analyzed data; J. Rudan Njavro, S.A. Müller and S.F. Lichtenthaler wrote the paper.

REFERENCES

1. Lichtenthaler SF, Lemberg MK, Fluhrer R. Proteolytic ectodomain shedding of membrane proteins in mammals-hardware, concepts, and recent developments. *EMBO J*. 2018;37:e99456.
2. Freeman M. The rhomboid-like superfamily: molecular mechanisms and biological roles. *Annu Rev Cell Dev Biol*. 2014;30:235-254.
3. Lemberg MK. Sampling the membrane: function of rhomboid-family proteins. *Trends Cell Biol*. 2013;23:210-217.
4. Johnson N, Brezinova J, Stephens E, et al. Quantitative proteomics screen identifies a substrate repertoire of rhomboid protease RHBDL2 in human cells and implicates it in epithelial homeostasis. *Sci Rep*. 2017;7:7283. https://doi.org/10.1038/s41598-017-07556-3.
5. Pruessmeyer J, Ludwig A. The good, the bad and the ugly substrates for ADAM10 and ADAM17 in brain pathology, inflammation and cancer. *Semin Cell Dev Biol*. 2009;20:164-174.
6. Saftig P, Lichtenthaler SF. The alpha secretase ADAM10: a metalloprotease with multiple functions in the brain. *Prog Neurogibol*. 2015;135:1-20.
7. Weber S, Saftig P. Ectodomain shedding and ADAMs in development. *Development*. 2012;139:3693-3709.
8. Zunke F, Rose-John S. The shedding protease ADAM17: Physiology and pathophysiology. *Biochim Biophys Acta Mol Cell Res*. 2017;1864:2059-2070.
9. Kuhn PH, Voss M, Haug-Kroper M, et al. Secretome analysis identifies novel signal Peptide peptidase-like 3 (Sppl3) substrates and reveals a role of Sppl3 in multiple Golgi glycosylation pathways. *Mol Cell Proteomics*. 2015;14:1584-1598.
10. Voss M, Kunzel U, Higel F, et al. Shedding of glycan-modifying enzymes by signal peptide peptidase-like 3 (SPPL3) regulates cellular N-glycosylation. *EMBO J*. 2014;33:2890-2905.
11. Kuhn PH, Koroniak K, Hogl S, et al. Secretome protein enrichment identifies physiological BACE1 protease substrates in neurons. *EMBO J*. 2012;31:3157-3168.
12. Stutzer I, Selevsek N, Esterhazy D, Schmidt A, Aebersold R, Stoffel M. Systematic proteomic analysis identifies beta-site amyloid precursor protein cleaving enzyme 2 and 1 (BACE2 and BACE1) substrates in pancreatic beta-cells. *J Biol Chem*. 2013;288:10536-10547.
13. Hemming ML, Elias JE, Gygi SP, Selkoe DJ. Identification of beta-secretase (BACE1) substrates using quantitative proteomics. *PLoS ONE*. 2009;4:e8477.
14. Zhou L, Barao S, Laga M, et al. The neural cell adhesion molecules L1 and CHL1 are cleaved by BACE1 protease in vivo. *J Biol Chem*. 2012;287:25927-25940.
15. Dislich B, Wohlrab F, Bachhuber T, et al. Label-free quantitative proteomics of mouse cerebrospinal fluid detects beta-site APP cleaving enzyme (BACE1) protease substrates in vivo. *Mol Cell Proteomics*. 2015;14:2550-2563.
16. Voytyuk I, Mueller SA, Herber J, et al. BACE2 distribution in major brain cell types and identification of novel substrates. *Life Sci Alliance*. 2018;1:e201800026.
17. Vassar R, Bennett BD, Babu-Khan S, et al. Beta-secretase cleavage of Alzheimer's amyloid precursor protein by the transmembrane aspartic protease BACE. *Science*. 1999;286:735-741.
18. Hardy J, Selkoe DJ. The amyloid hypothesis of Alzheimer's disease: progress and problems on the road to therapeutics. *Science*. 2002;297:353-356.
19. Volloch V, Rits S. Results of beta secretase-inhibitor clinical trials support amyloid precursor protein-independent generation of beta amyloid in sporadic Alzheimer's disease. *Med Sci (Basel, Switzerland)*. 2018;6:E45.
20. Egan MF, Kost J, Voss T, et al. Randomized trial of verubecestat for prodromal Alzheimer's disease. *N Engl J Med*. 2019;380:1408-1420.
21. Egan MF, Kost J, Tariot PN, et al. Randomized trial of verubecestat for mild-to-moderate Alzheimer's disease. *N Engl J Med*. 2018;378:1691-1703.
22. Henley D, Raghavan N, Sperling R, Aisen P, Raman R, Romano G. Preliminary results of a trial of atabecestat in preclinical Alzheimer's disease. *N Engl J Med*. 2019;380:1483-1485.
23. Barao S, Moechars D, Lichtenthaler SF, De Strooper B. BACE1 physiological functions may limit its use as therapeutic target for Alzheimer's disease. *Trends Neurosci*. 2016;39:158-169.
24. Cheret C, Willem M, Fricker FR, et al. Bace1 and Neuregulin-1 cooperate to control formation and maintenance of muscle spindles. *EMBO J*. 2013;32:2015-2028.
25. Willem M, Garratt AN, Novak B, et al. Control of peripheral nerve myelination by the beta-secretase BACE1. *Science*. 2006;314:664-666.
26. Hu X, Hicks CW, He W, et al. Bace1 modulates myelination in the central and peripheral nervous system. *Nat Neurosci*. 2006;9:1520-1525.

27. Gunnersen JM, Kim MH, Fuller SJ, et al. Sez-6 proteins affect dendritic arborization patterns and excitability of cortical pyramidal neurons. *Neuron*. 2007;56:621-639.
28. Zhu K, Xiang X, Filser S, et al. Beta-site amyloid precursor protein cleaving enzyme 1 inhibition impairs synaptic plasticity via seizure protein 6. *Biol Psychiatry*. 2018;83:428-437.
29. Vnencak M, Scholvinck ML, Schwarzacher SW, Deller T, Willem M, Jedlicka P. Lack of beta-amyloid cleaving enzyme-1 (BACE1) impairs long-term synaptic plasticity but enhances granule cell excitability and oscillatory activity in the dentate gyrus in vivo. *Brain Struct Funct*. 2019;224:1279–1290.
30. Hitt B, Riordan SM, Kukreja L, Eimer WA, Rajapaksha TW, Vassar R. beta-Site amyloid precursor protein (APP)-cleaving enzyme 1 (BACE1)-deficient mice exhibit a close homolog of L1 (CHL1) loss-of-function phenotype involving axon guidance defects. *J Biol Chem*. 2012;287:38408-38425.
31. Ou-Yang MH, Kurz JE, Nomura T, et al. Axonal organization defects in the hippocampus of adult conditional BACE1 knockout mice. *Sci Transl Med*. 2018;10:eaao5620.
32. Hu X, He W, Luo X, Tsubota KE, Yan R. BACE1 regulates hippocampal astrogenesis via the Jagged1-Notch pathway. *Cell Rep*. 2013;4:40-49.
33. Ohno M, Sametsky EA, Younkin LH, et al. BACE1 deficiency rescues memory deficits and cholinergic dysfunction in a mouse model of Alzheimer's disease. *Neuron*. 2004;41:27-33.
34. Ohno M, Chang L, Tseng W, et al. Temporal memory deficits in Alzheimer's mouse models: rescue by genetic deletion of BACE1. *Eur J Neuorsci*. 2006;23:251-260.
35. Ohno M, Cole SL, Yasvoina M, et al. BACE1 gene deletion prevents neuron loss and memory deficits in 5XFAD APP/PS1 transgenic mice. *Neurobiol Dis*. 2007;26:134-145.
36. Laird FM, Cai H, Savonenko AV, et al. BACE1, a major determinant of selective vulnerability of the brain to amyloid-beta amyloidogenesis, is essential for cognitive, emotional, and synaptic functions. *J Neurosci*. 2005;25:11693-11709.
37. Harrison SM, Harper AJ, Hawkins J, et al. BACE1 (beta-secretase) transgenic and knockout mice: identification of neurochemical deficits and behavioral changes. *Mol Cell Neurosci*. 2003;24:646-655.
38. Dominguez D, Tournoy J, Hartmann D, et al. Phenotypic and biochemical analyses of BACE1- and BACE2-deficient mice. *J Biol Chem*. 2005;280:30797-30806.
39. Vassar R. Editorial: implications for BACE1 inhibitor clinical trials: adult conditional BACE1 knockout mice exhibit axonal organization defects in the hippocampus. *J Prev Alzheimer's Dis*. 2019;6:78-84.
40. Cai H, Wang Y, McCarthy D, et al. BACE1 is the major beta-secretase for generation of Abeta peptides by neurons. *Nat Neurosci*. 2001;4:233-234.
41. Wisniewski JR, Zougman A, Nagaraj N, Mann M. Universal sample preparation method for proteome analysis. *Nat Methods*. 2009;6:359-362.
42. Rappsilber J, Mann M, Ishihama Y. Protocol for micro-purification, enrichment, pre-fractionation and storage of peptides for proteomics using StageTips. *Nat Protoc*. 2007;2:1896-1906.
43. Wisniewski JR, Zougman A, Mann M. Combination of FASP and StageTip-based fractionation allows in-depth analysis of the hippocampal membrane proteome. *J Proteome Res*. 2009;8:5674-5678.
44. Cox J, Hein MY, Luber CA, Paron I, Nagaraj N, Mann M. Accurate proteome-wide label-free quantification by delayed normalization and maximal peptide ratio extraction, termed MaxLFQ. *Mol Cell Proteomics*. 2014;13:2513-2526.
45. Tyanova S, Temu T, Sinitcyn P, et al. The Perseus computational platform for comprehensive analysis of (prote)omics data. *Nat Methods*. 2016;13:731-740.
46. Tusher VG, Tibshirani R, Chu G. Significance analysis of microarrays applied to the ionizing radiation response. *Proc Natl Acad Sci U S A*. 2001;98:5116-5121.
47. Pigoni M, Wanngren J, Kuhn PH, et al. Seizure protein 6 and its homolog seizure 6-like protein are physiological substrates of BACE1 in neurons. *Mol Neurodegener*. 2016;11:67. https://doi.org/10.1186/s13024-016-0134-z.
48. Kohler G, Milstein C. Continuous cultures of fused cells secreting antibody of predefined specificity. *Nature*. 1975;256:495-497.
49. Mitterreiter S, Page RM, Kamp F, et al. Bepridil and amiodarone simultaneously target the Alzheimer's disease beta- and gamma-secretase via distinct mechanisms. *J Neurosci*. 2010;30:8974-8983.
50. Colombo A, Wang H, Kuhn PH, et al. Constitutive alpha- and beta-secretase cleavages of the amyloid precursor protein are partially coupled in neurons, but not in frequently used cell lines. *Neurobiol Dis*. 2013;49:137-147.
51. Kuhn PH, Colombo AV, Schusser B. Systematic substrate identification indicates a central role for the metalloprotease ADAM10 in axon targeting and synapse function. *eLife*. 2016;5:e12748.
52. Hitz C, Wurst W, Kuhn R. Conditional brain-specific knockdown of MAPK using Cre/loxP regulated RNA interference. *Nucleic Acids Res*. 2007;35:e90.
53. Ingold I, Berndt C, Schmitt S, et al. Selenium utilization by GPX4 is required to prevent hydroperoxide-induced ferroptosis. *Cell*. 2018;172:409-422.e421.
54. Vlachos A, Ikenberg B, Lenz M, et al. Synaptopodin regulates denervation-induced homeostatic synaptic plasticity. *Proc Natl Acad Sci U S A*. 2013;110:8242-8247.
55. Michalakis S, Geiger H, Haverkamp S, Hofmann F, Gerstner A, Biel M. Impaired opsin targeting and cone photoreceptor migration in the retina of mice lacking the cyclic nucleotide-gated channel CNGA3. *Invest Ophthalmol Vis Sci*. 2005;46:1516-1524.
56. Pastorino L, Ikin AF, Lamprianou S, et al. BACE (beta-secretase) modulates the processing of APLP2 in vivo. *Mol Cell Neurosci*. 2004;25:642-649.
57. Hogl Sebastian, van Bebber Frauke, Dislich Bastian, Kuhn Peer-Hendrik, Haass Christian, Schmid Bettina, Lichtenthaler Stefan F. Label-free quantitative analysis of the membrane proteome of Bace1 protease knock-out zebrafish brains. *PROTEOMICS*. 2013;13:1519-1527.
58. Dahimene S, Page KM, Kadurin I, et al. The alpha2delta-like protein Cachd1 increases N-type calcium currents and cell surface expression and competes with alpha2delta-1. *Cell Rep*. 2018;25:1610-1621.e1615.
59. Cottrell GS, Soubrane CH, Hounshell JA, et al. CACHD1 is an alpha2delta-like protein that modulates CaV3 voltage-gated calcium channel activity. *J Neurosci*. 2018;38:9186-9201.
60. Stachel SJ, Coburn CA, Steele TG, et al. Structure-based design of potent and selective cell-permeable inhibitors of human beta-secretase (BACE-1). *J Med Chem*. 2004;47:6447-6450.
61. May PC, Willis BA, Lowe SL, et al. The potent BACE1 inhibitor LY2886721 elicits robust central Abeta pharmacodynamic responses in mice, dogs, and humans. *J Neurosci*. 2015;35:1199-1210.

62. Sherrington R, Rogaev EI, Liang Y, et al. Cloning of a gene bearing missense mutations in early-onset familial Alzheimer's disease. *Nature*. 1995;375:754-760.
63. De Strooper B, Saftig P, Craessaerts K, et al. Deficiency of presenilin-1 inhibits the normal cleavage of amyloid precursor protein. *Nature*. 1998;391:387-390.
64. Wolfe MS, Xia W, Ostaszewski BL, Diehl TS, Kimberly WT, Selkoe DJ. Two transmembrane aspartates in presenilin-1 required for presenilin endoproteolysis and gamma-secretase activity. *Nature*. 1999;398:513-517.
65. Dovey HF, John V, Anderson JP, et al. Functional gamma-secretase inhibitors reduce beta-amyloid peptide levels in brain. *J Neurochem*. 2001;76:173-181.
66. Gruninger-Leitch F, Schlatter D, Kung E, Nelbock P, Dobeli H. Substrate and inhibitor profile of BACE (beta-secretase) and comparison with other mammalian aspartic proteases. *J Biol Chem*. 2002;277:4687-4693.
67. Wang H, Megill A, Wong PC, Kirkwood A, Lee HK. Postsynaptic target specific synaptic dysfunctions in the CA3 area of BACE1 knockout mice. *PLoS ONE*. 2014;9:e92279.
68. Nguyen QA, Horn ME, Nicoll RA. Distinct roles for extracellular and intracellular domains in neuroligin function at inhibitory synapses. *eLife*. 2016;5:e19236.
69. Connor SA, Elegheert J, Xie Y, Craig AM. Pumping the brakes: suppression of synapse development by MDGA-neuroligin interactions. *Curr Opin Neurobiol*. 2019;57:71-80.
70. Cai J, Qi X, Kociok N, et al. beta-Secretase (BACE1) inhibition causes retinal pathology by vascular dysregulation and accumulation of age pigment. *EMBO Mol Med*. 2012;4:980-991.
71. Ishikawa T, Gotoh N, Murayama C, et al. IgSF molecule MDGA1 is involved in radial migration and positioning of a subset of cortical upper-layer neurons. *Dev Dyn*. 2011;240:96-107.
72. Takeuchi A, O'Leary DD. Radial migration of superficial layer cortical neurons controlled by novel Ig cell adhesion molecule MDGA1. *J Neurosci*. 2006;26:4460-4464.
73. Pettem KL, Yokomaku D, Takahashi H, Ge Y, Craig AM. Interaction between autism-linked MDGAs and neuroligins suppresses inhibitory synapse development. *J Cell Biol*. 2013;200:321-336.
74. Lee K, Kim Y, Lee SJ, et al. MDGAs interact selectively with neuroligin-2 but not other neuroligins to regulate inhibitory synapse development. *Proc Natl Acad Sci U S A*. 2013;110:336-341.
75. Connor SA, Ammendrup-Johnsen I, Kishimoto Y, et al. Loss of synapse repressor MDGA1 enhances perisomatic inhibition, confers resistance to network excitation, and impairs cognitive function. *Cell Rep*. 2017;21:3637-3645.
76. Kim JA, Kim D, Won SY, et al. Structural insights into modulation of neurexin-neuroligin trans-synaptic adhesion by MDGA1/neuroligin-2 complex. *Neuron*. 2017;94:1121-1131.e1126.
77. Gangwar SP, Zhong X, Seshadrinathan S, Chen H, Machius M, Rudenko G. Molecular mechanism of MDGA1: regulation of neuroligin 2: neurexin trans-synaptic Bridges. *Neuron*. 2017;94:1132-1141.e1134.
78. Kim DY, Carey BW, Wang H, et al. BACE1 regulates voltage-gated sodium channels and neuronal activity. *Nat Cell Biol*. 2007;9:755-764.
79. Wong HK, Sakurai T, Oyama F, et al. beta Subunits of voltage-gated sodium channels are novel substrates of beta-site amyloid precursor protein-cleaving enzyme (BACE1) and gamma-secretase. *J Biol Chem*. 2005;280:23009-23017.
80. Wu J, Yan Z, Li Z, et al. Structure of the voltage-gated calcium channel Ca(v)1.1 at 3.6 A resolution. *Nature*. 2016;537:191-196.
81. Jay SD, Sharp AH, Kahl SD, Vedvick TS, Harpold MM, Campbell KP. Structural characterization of the dihydropyridine-sensitive calcium channel alpha 2-subunit and the associated delta peptides. *J Biol Chem*. 1991;266:3287-3293.
82. De Jongh KS, Warner C, Catterall WA. Subunits of purified calcium channels. Alpha 2 and delta are encoded by the same gene. *J Biol Chem*. 1990;265:14738-14741.
83. Gordon WR, Arnett KL, Blacklow SC. The molecular logic of Notch signaling—a structural and biochemical perspective. *J Cell Sci*. 2008;121:3109-3119.
84. Brummer T, Muller SA, Pan-Montojo F, et al. NrCAM is a marker for substrate-selective activation of ADAM10 in Alzheimer's disease. *EMBO Mol Med*. 2019;11:e9695.
85. Ullrich A, Bell JR, Chen EY, et al. Human insulin receptor and its relationship to the tyrosine kinase family of oncogenes. *Nature*. 1985;313:756-761.
86. Ebina Y, Ellis L, Jarnagin K, et al. The human insulin receptor cDNA: the structural basis for hormone-activated transmembrane signalling. *Cell*. 1985;40:747-758.
87. Colombo A, Hsia HE, Wang M, et al. Non-cell-autonomous function of DR6 in Schwann cell proliferation. *EMBO J*. 2018;37:e97390.
88. Haapasalo A, Kovacs DM. The many substrates of presenilin/gamma-secretase. *J Alzheimers Dis*. 2011;25:3-28.
89. Oikawa N, Walter J. Presenilins and gamma-secretase in membrane proteostasis. *Cells*. 2019;8:E209.
90. Herber J, Njavro J, Feederle R, et al. Click chemistry-mediated biotinylation reveals a function for the protease BACE1 in modulating the neuronal surface glycoproteome. *Mol Cell Proteomics*. 2018;17:1487–1501.
91. Li J, Liu J, Feng G, et al. The MDGA1 gene confers risk to schizophrenia and bipolar disorder. *Schizophr Res*. 2011;125:194-200.
92. Kahler AK, Djurovic S, Kulle B, et al. Association analysis of schizophrenia on 18 genes involved in neuronal migration: MDGA1 as a new susceptibility gene. *Am J Med Genet B Neuropsychiatr Genet*. 2008;147b:1089-1100.

SUPPORTING INFORMATION

Additional supporting information may be found online in the Supporting Information section.

How to cite this article: Njavro JR, Klotz J, Dislich B, et al. Mouse brain proteomics establishes MDGA1 and CACHD1 as in vivo substrates of the Alzheimer protease BACE1. *The FASEB Journal*. 2019;00:1–18. https://doi.org/10.1096/fj.201902347R